

The Spectrum of Hot Water: Rotational Transitions and Difference Bands in the (020), (100), and (001) Vibrational States

Oleg L. Polyansky,^{*,1} Jonathan Tennyson,^{*} and Peter F. Bernath^{†,2}

^{*}Department of Physics and Astronomy, University College London, Gower Street, London WC1E 6BT, United Kingdom;
and [†]Departments of Chemistry and Physics, University of Waterloo, Waterloo, Ontario, Canada N2L 3G1

Received March 24, 1997; in revised form July 17, 1997

Analysis of the hot H₂¹⁶O spectrum, presented by Polyansky *et al.* (1996, *J. Mol. Spectrosc.* **176**, 305–315), is extended to higher vibrational states. Three hundred thirty mainly strong lines are assigned to pure rotational transitions in the (100), (001), and (020) vibrational states. These lines, which involve significantly higher rotational energy levels than were known previously, are assigned using high-accuracy variational calculations. Transitions in (020) are assigned up to $K_a = 18$, compared with the maximum K_a of 10 known previously. Crossings of vibration–rotation energy levels result in the observation of extra intensity-stealing transitions. In particular, this leads to the assignment of (020)–(100) and (100)–(020) rotational difference band transitions in addition to the conventional pure rotational lines in (020) and (100) states. These extra lines increase the number of transitions and they are likely to complicate the pure rotational water spectrum in higher excited vibrational states to an even greater extent. A few lines from our previous work on the pure rotational spectrum of hot water in the (000) and (010) vibrational states are also reassigned and some further assignments are made. © 1997 Academic Press

I. INTRODUCTION

The spectrum of hot water has a number of important applications but presents a major experimental and theoretical challenge. For example, detailed high-resolution spectra of sunspots covering a large range in the infrared have been observed (1, 2). These dense spectra are almost totally unassigned. In order to assign this spectrum and other hot water spectra we have been analyzing the laboratory spectra of hot H₂¹⁶O.

In a recent paper, henceforth known as I, Polyansky *et al.* (3) presented measurements of the 1550°C water spectrum in the region 400–900 cm⁻¹. More than 4000 lines were observed and about 600 were assigned as lines belonging to pure rotational transitions in the (000) and (010) vibrational states. At least 300 very strong lines remained unassigned.

The assignments in I were made using a Padé–Borel effective Hamiltonian (4) and a procedure suitable only for working with isolated vibrational states. The accuracy of the prediction of the highest rotational energy levels was about 2 cm⁻¹, which was not sufficient for a complete analysis of a spectrum with a line density of about 15 lines per cm⁻¹. One reason for this low accuracy was the relatively small number of constants used to fit the data.

As pointed out in I, a natural method for analyzing the data which involves tens of vibrational states is a variational

calculation using a highly accurate potential energy surface (5–8). Thus, for example, Polyansky *et al.* (5) performed a variational fit to energy levels with J less than 15, but obtained excellent agreement with the highest observed levels up to $J = 35$. When we used variational calculations in the analysis of the ν_2 manifold, we were able to greatly extend the range of both J and K_a levels. In addition we detected transitions in the previously unknown $5\nu_2 - 4\nu_2$ band (9).

The motivation for the present work was to assign the remaining strong transitions in the water spectrum presented in I. These assignments are needed to provide a basis for the analysis of the many weaker lines also present. An understanding of both strong and weak lines is necessary to understand the very dense hot water spectrum in sunspots (1, 2). As will be shown, these assignments significantly extend our knowledge of the excited energy levels of water in the ground and excited vibrational states.

The extension of the water energy levels to high values of K_a is well known to be particularly difficult. Levels with high K_a are very sensitive to the small angle regions of the potential energy surface which are relatively poorly characterized by the available experimental data (5, 6). The high K_a levels are also strongly affected by adiabatic effects due to the breakdown of the Born–Oppenheimer approximation (7).

In this work, we extend K_a assignments for (010) from 19 (given in I) to 21; for (001) the highest derived K_a is now 20, compared to 16 given by Flaud *et al.* (10); for the ground and (100) vibrational states we increase K_a to 24 from 23 (in I) and to 20 from 19 (10), respectively. A major advance has been made for the (020) state where the highest

¹ Permanent address: Institute of Applied Physics, Russian Academy of Science, Uljanov Street 46, Nizhni Novgorod, Russia 603024.

² Also: Department of Chemistry, University of Arizona, Tucson, AZ 85721.

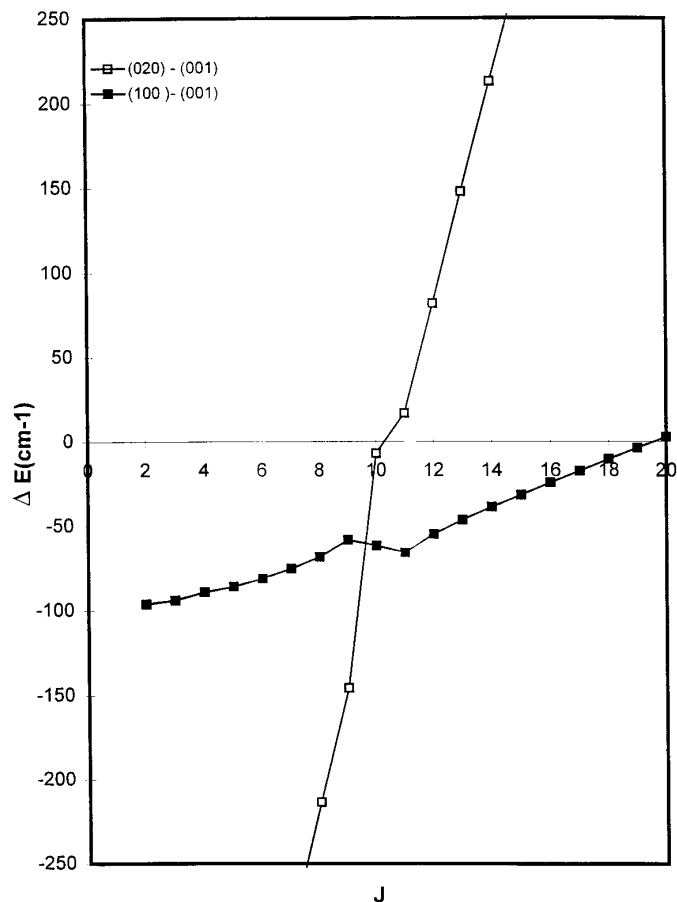


FIG. 1. Energy levels with $J = K_a$ as a function of J for the (001), (020), and (001) vibrational states. For each value of J , the zero of energy is taken as the J_{J_0} level of the (001) state.

observed K_a has been extended from 10, in Refs. (11, 12), to 18. This jump was made possible by the observation of difference band transitions, starting at $J \sim 10$. These difference band transitions were not recognized previously and had served as a barrier to further assignments. A number of linked phenomena occur in this region: crossings between levels of the (020) state and (100) state, intensity stealing because of the near degeneracy of the rotational energies, and mixing of the wavefunctions of the two different vibrational states. We also find other, more localized crossings which lead to a number of difference band transitions.

Although difference bands are by no means a new phenomenon, they are rare for pure rotational spectra. Previous examples are known for acetylene and diacetylene where, for example, the difference between two bending modes is seen at 2.4 cm^{-1} for HC_4H (13). We label these bands rotational difference bands and note that they have the unusual property that the vibrational states involved can appear as both the "upper" and the "lower" state in the same spectrum. We show that these rotational difference bands have the useful property that their assignments are self-con-

firmed and suggest that such transitions will be common in the spectra of hot molecules.

II. ANALYSIS

The experimental details of the observation of the hot water spectrum at 1550°C have been described in I. Here we use the transition frequencies and intensities reported there.

The analysis in the present study, as in Ref. (9), has been carried out using variational calculations of the water energy levels (7) which employed a preliminary fit to the highly accurate, *ab initio* Born–Oppenheimer potential energy surface calculations of Partridge and Schwenke (8). Effects beyond the Born–Oppenheimer approximation were accounted for by an *ab initio* adiabatic surface (7) as well as the use of masses halfway between nuclear and atomic

TABLE 1
Pure Rotational and Rotational Difference Band Lines Involving $K_a = 10$ Levels Which Are Heavily Mixed for the (020) and (100) Vibrational States

Wavenumber	Intensity	J'	K'_a	K'_c	J	K_a	K_c	$v'_1 v'_2 v'_3 - v_1 v_2 v_3$
427.76010	.0964	10	10	1	9	9	0	100 - 100
454.19827	.0753	11	10	1	10	9	2	100 - 100
479.79149	.0653	12	10	3	11	9	2	100 - 100
481.93279	.2583	10	10	1	9	9	0	020 - 100
504.48308	.0933	13	10	3	12	9	4	100 - 100
509.43603	.2682	11	10	1	10	9	2	020 - 100
514.82675	.2062	10	10	1	9	9	0	100 - 020
528.24932	.0735	14	10	5	13	9	4	100 - 100
536.84045	.2802	12	10	3	11	9	2	020 - 100
537.53842	.2593	11	10	1	10	9	2	100 - 020
551.09870	.0567	15	10	5	14	9	6	100 - 100
559.52798	.1908	12	10	3	11	9	2	100 - 020
564.00715	.2293	13	10	3	12	9	4	020 - 100
568.99962	.1655	10	10	1	9	9	0	020 - 020
573.03214	.0545	16	10	7	15	9	6	100 - 100
573.05794	.0187	16	10	6	15	9	7	100 - 100
580.84027	.2818	13	10	3	12	9	4	100 - 020
590.78122	.2873	14	10	5	13	9	4	020 - 100
592.77633	.1874	11	10	1	10	9	2	020 - 020
601.53934	.3008	14	10	5	13	9	4	100 - 020
616.57740	.1939	12	10	3	11	9	2	020 - 020
617.01081	.2307	15	10	5	14	9	6	020 - 100
621.70268	.1958	15	10	6	14	9	5	100 - 020
640.36442	.1969	13	10	3	12	9	4	020 - 020
641.38289	.1957	16	10	7	15	9	6	100 - 020
641.40047	.0714	16	10	6	15	9	7	100 - 020
642.52374	.1924	16	10	7	15	9	6	020 - 100
642.54939	.0691	16	10	6	15	9	7	020 - 100
664.07128	.1735	14	10	5	13	9	4	020 - 020
687.61330	.1210	15	10	6	14	9	5	020 - 020
710.87412	.0843	16	10	7	15	9	6	020 - 020
710.89178	.0324	16	10	6	15	9	7	020 - 020

Note. Wavenumbers are in cm^{-1} and intensities in arbitrary relative units.

TABLE 2
Rotational Difference Band Lines Involving Isolated Interactions

J'	K'_a	K'_c	$(v'_1 v'_2 v'_3)$	J	K_a	K_c	$(v_1 v_2 v_3)$	E_{up}	E_{low}	F_{calc}	F_{obs}	I	
13	3	10	(020)	-	12	2	11	(020)	5654.762	4967.491	687.271	687.270	0.067
13	1	12	(100)	-	12	2	11	(020)	5662.478	4967.491	694.987	694.985	0.029
12	5	8	(020)	-	11	2	9	(020)	5587.519	4905.650	681.869	681.869	0.116
12	3	10	(100)	-	11	2	9	(020)	5579.492	4905.650	673.842	673.836	0.045
12	2	10	(020)	-	11	1	11	(020)	5182.095	4469.796	712.299	712.299	0.03
12	0	12	(100)	-	11	1	11	(020)	5186.339	4469.796	716.543	716.541	0.04
9	6	3	(020)	-	8	5	4	(020)	4996.331	4564.034	432.297	432.297	0.114
9	4	5	(100)	-	8	5	4	(020)	4992.122	4564.034	428.088	428.087	0.064

Note. These transitions were assigned on the basis of mixing as given in Ref. (14). All energies and transition frequencies are in cm⁻¹ and intensities (I) in arbitrary relative units.

masses for the H atoms to partially allow for nonadiabatic effects (7).

As in our analysis of the ν_2 manifold, we define trivial assignments as those for which experimental energy levels are known from previous work. We started our analysis by making all possible trivial assignments to the rotational spectrum in the (100) and (001) vibrational states, using the levels determined by Flaud *et al.* (10). Frustratingly, we were unable to make trivial assignments for lines of (100) and (020) with K_a higher than 9. Lines involving $K_a = 10$ were unexpectedly found to be of much lower intensity. Assignments, however, for the corresponding lines of (001) were made without any problems.

At this point we found that assignments could be made using the variational calculations. In this case we concentrated on the strong transitions in the original spectrum which were generally separated by 1 to 2 cm⁻¹. Typically the positions of these strong transitions were estimated with an accuracy of ~ 0.2 cm⁻¹ by the variational calculations, which is close enough to make assignments with confidence. As will be shown below, for some transitions it is possible to confirm these assignments using self-consistent criteria.

It was not possible to assign $K_a = 10$ levels for the (100) state using purely trivial assignments. This is because of the unexpected drop in intensity for transitions involving the previously published (10) (100) $K_a = 10$ levels, which we used for the trivial assignments. This implies that these rotational transitions do not, in fact belong to just the (100) state. It seemed that it was not possible to make trivial assignments beyond this K_a value. However, our analysis showed that for $K_a \geq 11$ it is indeed possible to continue making trivial assignments using the data of Flaud *et al.* These lines are again very strong as expected for rotational transitions belonging to the (100) vibrational state.

Our hypothesis was that there is intensity stealing between the (100) and (020) bands, since it is exactly at $K_a = 10$

that the (020) state energy levels with the same J begin to be higher than those of the (100) state. Figure 1 illustrates the relative position of the $K_a = J$ levels of the three vibrational states (020), (100), and (001) and the sharp break at $K_a = 10$ is clearly seen. It appears that this crossing of energy levels mixes the wavefunctions. Mixed wavefunctions mean that not only are pure rotational transitions within each vibrational manifold observable, but that the corresponding difference transitions linking the (100) and (020) states should also be seen. Furthermore, given the levels involved in the pure rotational transitions, the frequencies of the difference transitions become exactly determined and their observation serves as a direct confirmation of the identity of the interacting levels.

We checked for the occurrence of rotational difference bands, that is, the existence of not only (100)–(100) and (020)–(020) transitions, but also of the (100)–(020) and (020)–(100) transitions. The results given in Table 1 confirm their presence for $K_a = 10$. We also found somewhat weaker difference band transitions with $K_a = 9, 11,$ and $12,$ but failed to find any for other values of K_a .

Having found these rotational difference transitions we also decided to search for other energy level crossings that might lead to extra transitions. In fact Flaud and Camy-Peyret (14) had already noted states which were mixtures between (100) and (001) when analyzing the fundamental band spectra. Trivial analysis of these interacting states led us directly to other rotational difference transitions (see Table 2).

Once our analysis of the rotational difference bands was complete, we were certain that nothing mysterious happens to transitions with $K_a = 10$. The behavior of these lines can be explained by intensity stealing and the appearance of the rotational difference bands. We then proceeded with the assignment of higher J, K_a lines. We assigned lines with K_a as high as 20 for (100) and (001) and 18 for (020) vibrational states by comparison with the variational calculations.

TABLE 3
Pure Rotational Transitions in the (020)
Vibrational State in cm^{-1} with Intensities in
Arbitrary Relative Units

Wavenumber	Intensity	J'	K'_a	K'_c	J	K_a	K_c	$v_1 v_2 v_3$
402.92762	.0455	9	5	4	8	4	5	020
430.33745	.0828	9	6	4	8	5	3	020
432.29706	.1142	9	6	3	8	5	4	020
447.93624	.1160	14	5	10	13	4	9	020
454.48909	.0990	9	7	3	8	6	2	020
454.77432	.1613	9	7	2	8	6	3	020
477.47104	.1510	10	7	4	9	6	3	020
479.10916	.1494	10	7	3	9	6	4	020
488.44720	.2275	9	9	0	8	8	1	020
503.04183	.2686	11	7	4	10	6	5	020
503.97050	.1396	11	7	5	10	6	4	020
513.31479	.2476	10	9	2	9	8	1	020
523.36370	.0999	11	8	4	10	7	3	020
523.37368	.1928	11	8	3	10	7	4	020
523.94922	.1260	13	6	7	12	5	8	020
526.57398	.1309	12	7	5	11	6	6	020
526.90851	.2274	12	7	6	11	6	5	020
537.71093	.3026	11	9	2	10	8	3	020
547.12357	.2693	12	8	5	11	7	4	020
549.13416	.1549	13	7	7	12	6	6	020
549.79559	.2679	13	7	6	12	6	7	020
561.57586	.3041	12	9	4	11	8	3	020
570.12529	.2363	14	7	8	13	6	7	020
570.27123	.1579	13	8	6	12	7	5	020
570.38004	.3066	13	8	5	12	7	6	020
572.93060	.1594	14	7	7	13	6	8	020
577.02859	.3148	12	11	2	11	10	1	020
584.86201	.4005	13	9	4	12	8	5	020
592.71321	.3054	14	8	7	13	7	6	020
592.77634	.1874	11	10	1	10	9	2	020
596.51152	.3745	12	12	1	11	11	0	020
604.13539	.3679	13	11	2	12	10	3	020
607.52930	.3586	14	9	6	13	8	5	020
616.57741	.1939	12	10	3	11	9	2	020
622.69686	.3467	13	12	1	12	11	2	020
629.51775	.3193	15	9	6	14	8	7	020
630.42487	.3521	14	11	4	13	10	3	020
630.90551	.3678	13	13	0	12	12	1	020
640.36443	.1969	13	10	3	12	9	4	020
642.52375	.1924	16	10	7	15	9	6	020
642.54940	.0691	16	10	6	15	9	7	020
648.23328	.3482	14	12	3	13	11	2	020
655.87526	.3145	15	11	4	14	10	5	020
656.85540	.3284	14	13	2	13	12	1	020
661.48314	.3112	14	14	1	13	13	0	020
664.07130	.1735	14	10	5	13	9	4	020
673.10671	.2994	15	12	3	14	11	4	020
680.47261	.1825	16	11	6	15	10	5	020
682.11898	.2673	15	13	2	14	12	3	020
687.41608	.2347	15	14	1	14	13	2	020
687.61331	.1210	15	10	6	14	9	5	020
689.86602	.2132	15	15	0	14	14	1	020
697.30634	.2296	16	12	5	15	11	4	020
704.26119	.1465	17	11	6	16	10	7	020
706.69027	.1967	16	13	4	15	12	3	020
710.87413	.0843	16	10	7	15	9	6	020
712.57128	.2118	16	14	3	15	13	2	020
715.92466	.2178	16	15	2	15	14	1	020
716.52230	.1751	16	16	1	15	15	0	020
720.83577	.1720	17	12	5	16	11	6	020
730.56512	.2076	17	13	4	16	12	5	020
736.96095	.2012	17	14	3	16	13	4	020
741.10745	.1894	17	15	2	16	14	3	020
741.67661	.1309	17	17	0	16	16	1	020
742.47390	.1535	17	16	1	16	15	2	020
743.65212	.1527	18	12	7	17	11	6	020
753.73944	.1732	18	13	6	17	12	5	020
765.44732	.0956	18	15	4	17	14	3	020
765.48273	.0629	18	18	1	17	17	0	020
767.44653	.0818	18	16	3	17	15	2	020
767.65949	.0719	18	17	2	17	16	1	020
783.87351	.0835	14	4	11	13	1	12	020

This represents a significant improvement over previous work. Tables 3–5 present the pure rotational lines assigned to the (020), (100), and (001) vibrational states.

The assignments in I used a single vibrational state Padé–Borel effective Hamiltonian (4). We found that some of the lines reported in I were misassigned. We checked our assignments, particularly those pointed out to us as suspicious by Coudert (15), and found that the majority of the lines reported in I were assigned correctly. In particular all lines belonging to the ground vibrational states proved to be correct. About 10 lines from the (010) state, though, were suspicious. In each case alternative assignments have been found which agree significantly better with the variational calculations. They are presented in Table 6. Table 7 presents a number of new assignments that we were able to make for the (000) and (010) bands in the course of this work.

In paper I we presented tables of energy levels derived from the experimental data. Since some lines, starting with $J = 17$, turned out to be misassigned, the system of energy levels for the (010) state presented in I is incorrect for J higher than 16. Table 8 presents revised energy levels for the high K_a levels of the (010) state which are derived from the reassigned lines of Table 6 and the new assignments of Table 7.

III. DISCUSSION

Since at least some of the levels involved in the transitions reported in Table 2 were known (14) prior to our work, we expected to find pure rotational and rotational difference band transitions in standard compilations of water transitions such as HITRAN (16) and the water “atlas” (17). In fact, neither the pure rotational transitions nor the difference band lines are present in the atlas, and HITRAN contains only the pure rotational transitions. Thus, the major water line lists, widely used for spectral synthesis and modeling, do not contain these difference bands. It should be emphasized that although the cases listed in Table 2 are caused by isolated interactions, the (020)–(100) rotational difference band transitions given in Table 1 are not. Difference bands result in a doubling of the number of lines observed for all states with $J \geq K_a$ and K_a equal to 9, 10, 11, or 12.

Rotational difference band transitions arise naturally from any variational calculations based on a full Hamiltonian. It is therefore to be expected that they should occur in a variationally calculated database. Partridge and Schwenke (8) report a number of cases where they find extra lines in comparison with HITRAN. It would appear that most of these are rotational difference band transitions.

It may be thought that rotational difference band transitions are relatively weak, arising from small interactions. In many cases, particularly for the (020)–(100) lines with $K_a = 10$, this is not true; the intensity is fairly evenly distributed between all four possible transitions. This implies that the underlying wavefunctions are strongly mixed. In principle

TABLE 4
Pure Rotational Transitions in the (100) Vibrational State in cm⁻¹ with Intensities (Int) in Arbitrary Relative Units

Wavenumber	Intensity	J'	K'_a	K'_c	J	K_a	K_c	$v_1v_2v_3$	Wavenumber	Intensity	J'	K'_a	K'_c	J	K_a	K_c	$v_1v_2v_3$
390.55667	.0273	9	7	2	8	6	3	100	599.19062	.1860	16	9	8	15	8	7	100
411.11578	.0464	9	8	1	8	7	2	100	599.59096	.0829	16	9	7	15	8	8	100
414.16707	.0787	10	7	4	9	6	3	100	599.67036	.1089	18	8	11	17	7	10	100
414.24902	.0421	10	7	3	9	6	4	100	604.00340	.2882	14	14	1	13	13	0	100
427.06847	.0563	11	6	5	10	5	6	100	609.89121	.2601	15	11	4	14	10	5	100
435.42006	.1415	10	8	3	9	7	2	100	614.35182	.2563	15	12	3	14	11	4	100
437.20422	.0635	11	7	5	10	6	4	100	620.95686	.0550	17	9	9	16	8	8	100
437.49730	.1144	11	7	4	10	6	5	100	621.92323	.1418	17	9	8	16	8	9	100
454.19828	.0753	11	10	1	10	9	2	100	622.08825	.2684	15	13	2	14	12	3	100
455.59067	.1848	10	9	2	9	8	1	100	628.81664	.2378	15	14	1	14	13	2	100
459.35232	.0700	11	8	4	10	7	3	100	631.53283	.2263	16	11	6	15	10	5	100
459.37022	.1744	11	8	3	10	7	4	100	633.76374	.2586	15	15	0	14	14	1	100
460.22057	.0768	12	7	5	11	6	6	100	634.18954	.0240	19	10	9	18	9	10	100
479.79150	.0653	12	10	3	11	9	2	100	637.37406	.2469	16	12	5	15	11	4	100
480.20608	.0665	13	7	7	12	6	6	100	652.81675	.1816	17	11	6	16	10	7	100
480.50461	.2721	11	9	2	10	8	3	100	653.03685	.2246	16	14	3	15	13	2	100
482.17173	.1262	13	7	6	12	6	7	100	658.56386	.2292	16	15	2	15	14	1	100
482.81893	.2175	12	8	5	11	7	4	100	659.87476	.1788	17	12	5	16	11	6	100
502.15959	.0569	14	7	7	13	6	8	100	662.19624	.2170	16	16	1	15	15	0	100
504.48309	.0933	13	10	3	12	9	4	100	668.85806	.2069	17	13	4	16	12	5	100
505.12595	.2076	12	9	4	11	8	3	100	673.67134	.1314	18	11	8	17	10	7	100
505.69553	.1052	13	8	6	12	7	5	100	673.68935	.0467	18	11	7	17	10	8	100
515.21681	.0470	15	7	9	14	6	8	100	676.65341	.1401	17	14	3	16	13	4	100
520.85380	.1569	11	11	0	10	10	1	100	681.82806	.1487	18	12	7	17	11	6	100
527.78981	.1517	14	8	7	13	7	6	100	682.71463	.1381	17	15	2	16	14	3	100
528.24933	.0735	14	10	5	13	9	4	100	686.92849	.1454	17	16	1	16	15	2	100
529.39353	.0944	13	9	5	12	8	4	100	689.30277	.1298	17	17	0	16	16	1	100
529.40648	.1841	13	9	4	12	8	5	100	694.04329	.0327	19	11	9	18	10	8	100
542.47004	.2511	12	12	1	11	11	0	100	703.21101	.0964	19	12	7	18	11	8	100
543.40260	.2676	12	11	2	11	10	1	100	706.21151	.1052	18	15	4	17	14	3	100
546.49138	.1116	15	7	8	14	6	9	100	710.96140	.1145	18	16	3	17	15	2	100
548.79573	.0715	15	8	8	14	7	7	100	713.85925	.0766	20	11	10	19	10	9	100
550.46519	.2011	15	8	7	14	7	8	100	713.90889	.1080	18	17	2	17	16	1	100
551.09871	.0567	15	10	5	14	9	6	100	715.13516	.1013	18	18	1	17	17	0	100
553.28218	.0774	14	9	5	13	8	6	100	722.04437	.1190	19	14	5	18	13	6	100
565.77600	.3075	13	11	2	12	10	3	100	723.99326	.0792	20	12	9	19	11	8	100
566.86534	.3051	13	12	1	12	11	2	100	724.00359	.0235	20	12	8	19	11	9	100
568.23173	.1578	16	8	9	15	7	8	100	729.05456	.1085	19	15	4	18	14	5	100
571.90023	.0600	16	8	8	15	7	9	100	734.63213	.0971	20	13	8	19	12	9	100
573.03215	.0545	16	10	7	15	9	6	100	737.78079	.1324	19	17	2	18	16	3	100
573.05795	.0187	16	10	6	15	9	7	100	739.76190	.0657	19	19	0	18	18	1	100
573.12698	.3109	13	13	0	12	12	1	100	743.80958	.0877	20	14	7	19	13	6	100
576.55119	.0858	15	9	7	14	8	6	100	756.93531	.0690	20	16	5	19	15	4	100
576.69534	.2298	15	9	6	14	8	7	100	760.91265	.0591	20	17	4	19	16	3	100
587.95338	.2854	14	11	4	13	10	3	100	763.21643	.0475	20	18	3	19	17	2	100
594.09636	.0142	17	10	8	16	9	7	100	763.25375	.0457	20	20	1	19	19	0	100
594.17530	.0425	17	10	7	16	9	8	100	763.90530	.0392	20	19	2	19	18	1	100

it should be possible to use the intensity data to extract information on the degree of mixing. We tried to do this using simple mixing coefficients and the assumption that mixing occurred only in either the upper or the lower state.

However, in most cases it was not possible to get consistent solutions for such a model and we were forced to conclude that mixing occurs in all states involved in the transitions. We are currently addressing this problem using variational

TABLE 5
Pure Rotational Transitions in the (001) Vibrational State in cm^{-1} with Intensities in Arbitrary Relative Units

Wavenumber	Intensity	J'	K'_a	K'_c	J	K_a	K_c	$v_1v_2v_3$	Wavenumber	Intensity	J'	K'_a	K'_c	J	K_a	K_c	$v_1v_2v_3$
385.08222	.0161	9	7	3	8	6	2	001	584.75100	.1648	16	9	7	15	8	8	001
385.13168	.0178	9	7	2	8	6	3	001	590.04619	.3063	14	13	1	13	12	2	001
404.09059	.0500	9	8	2	8	7	1	001	593.63120	.2929	15	11	5	14	10	4	001
409.05770	.0534	10	7	3	9	6	4	001	596.44929	.3278	14	14	0	13	13	1	001
420.51708	.0986	9	9	0	8	8	1	001	601.85444	.0801	16	10	7	15	9	6	001
428.34922	.0452	10	8	3	9	7	2	001	601.93130	.2020	16	10	6	15	9	7	001
428.35777	.0702	10	8	2	9	7	3	001	605.33328	.2845	15	12	4	14	11	3	001
431.84097	.0806	11	7	5	10	6	4	001	614.69876	.2334	15	13	3	14	12	2	001
432.69282	.0423	11	7	4	10	6	5	001	616.62866	.2199	16	11	5	15	10	6	001
440.40026	.0843	12	6	6	11	5	7	001	621.77385	.2384	15	14	2	14	13	1	001
445.27573	.1526	10	9	1	9	8	2	001	623.57384	.1507	17	10	8	16	9	7	001
452.19376	.1221	11	8	4	10	7	3	001	623.79723	.0545	17	10	7	16	9	8	001
452.23772	.0587	11	8	3	10	7	4	001	626.52562	.2116	15	15	1	14	14	0	001
453.70456	.1051	12	7	6	11	6	5	001	628.85122	.2119	16	12	4	15	11	5	001
456.22021	.1435	12	7	5	11	6	6	001	638.75859	.2893	16	13	3	15	12	4	001
459.46398	.1493	10	10	0	9	9	1	001	639.02456	.1733	17	11	7	16	10	6	001
469.68546	.2661	11	9	3	10	8	2	001	639.04045	.0640	17	11	6	16	10	7	001
473.65937	.1266	13	7	7	12	6	6	001	645.08102	.1279	18	10	8	17	9	9	001
480.06086	.0542	13	7	6	12	6	7	001	646.44668	.2077	16	14	2	15	13	3	001
484.34758	.2581	11	10	2	10	9	1	001	651.78229	.2200	17	12	6	16	11	5	001
490.72201	.0453	14	7	8	13	6	7	001	651.95029	.1918	16	15	1	15	14	2	001
493.68549	.2629	12	9	3	11	8	4	001	655.01943	.1726	16	16	0	15	5	1	001
496.43083	.2527	11	11	1	10	10	0	001	660.78920	.0444	18	11	8	17	10	7	001
498.08376	.1611	13	8	6	12	7	5	001	660.83717	.1199	18	11	7	17	10	8	001
498.64782	.1215	13	8	5	12	7	6	001	662.20931	.1968	17	13	5	16	12	4	001
504.00003	.0833	15	7	9	14	6	8	001	670.46186	.1884	17	14	4	16	13	3	001
504.94479	.1253	14	7	7	13	6	8	001	674.10567	.1447	18	12	6	17	11	7	001
508.84049	.2552	12	10	2	11	9	3	001	676.64111	.1401	17	15	3	16	14	2	001
517.18935	.1398	13	9	5	12	8	4	001	680.40412	.1244	17	16	2	16	15	1	001
517.22420	.0637	13	9	4	12	8	5	001	682.37050	.1071	17	17	1	16	16	0	001
519.64601	.0400	14	8	7	13	7	6	001	685.03722	.1249	18	13	5	17	12	6	001
521.23224	.1134	14	8	6	13	7	7	001	693.81949	.1222	18	14	4	17	13	5	001
521.43743	.1877	12	11	1	11	10	2	001	695.79526	.0851	19	12	8	18	11	7	001
531.51382	.2280	12	12	0	11	11	1	001	700.60676	.1104	18	15	3	17	14	4	001
531.94374	.0505	15	7	8	14	6	9	001	704.95731	.0924	18	16	2	17	15	3	001
532.88957	.2233	13	10	4	12	9	3	001	707.23074	.0951	19	13	7	18	12	6	001
539.72516	.1445	15	8	8	14	7	7	001	707.97716	.1003	18	17	2	17	16	1	001
540.13150	.1172	14	9	6	13	8	5	001	708.29554	.0873	18	18	0	17	17	1	001
540.24932	.1976	14	9	5	13	8	6	001	716.50687	.1238	19	14	6	18	13	5	001
543.64491	.0561	15	8	7	14	7	8	001	716.83014	.0251	20	12	9	19	11	8	001
546.00021	.2531	13	11	3	12	10	2	001	716.88144	.0702	20	12	8	19	11	9	001
556.44824	.2537	14	10	4	13	9	5	001	723.85818	.1038	19	15	5	18	14	4	001
556.63563	.2569	13	12	2	12	11	1	001	728.78017	.0893	19	16	4	18	15	3	001
562.38452	.2650	15	9	7	14	8	6	001	733.06331	.0640	19	19	1	18	18	0	001
562.74765	.0712	15	9	6	14	8	7	001	733.84641	.0771	19	18	2	18	17	1	001
564.81723	.2814	13	13	1	12	12	0	001	738.53004	.0827	20	14	6	19	13	7	001
566.31663	.1052	16	8	8	15	7	9	001	746.40039	.0829	20	15	5	19	14	6	001
570.07758	.2339	14	11	3	13	10	4	001	751.69149	.0730	20	16	4	19	15	5	001
579.45214	.2015	15	10	6	14	9	5	001	756.23342	.0570	20	17	3	19	16	4	001
579.47572	.0781	15	10	5	14	9	6	001	756.73765	.0435	20	20	0	19	19	1	001
581.25268	.2889	14	12	2	13	11	3	001	758.34805	.0486	20	18	2	19	17	3	001

TABLE 6
Reassigned Transitions from Ref. (3)

Wavenumber	Intensity	J'	K'_a	K'_c	J	K_a	K_c	$v_1v_2v_3$
449.27890a	.2260	8	8	1	7	7	0	020
449.36785	.0639	23	7	16	22	8	15	000
496.14024	.1367	17	6	12	16	5	11	010
496.39507a	.1536	20	6	15	19	5	14	010
493.68548a	.2629	12	9	3	11	8	4	001
517.18934a	.1398	13	9	5	12	8	4	001
518.78710a	.1481	25	4	21	24	5	20	000
520.13515a	.1825	24	6	19	23	5	18	000
549.15711a	.3280	11	11	0	10	10	1	020
549.54074	.1678	24	7	18	23	6	17	000
576.61892	.1971	17	7	11	16	6	10	010
576.69533a	.2298	15	9	6	14	8	7	100
579.53254	.1813	20	7	14	19	6	13	010
580.84027b	.2818	13	10	3	12	9	4	100-020
581.00694b	.2796	18	7	12	17	6	11	010
581.25267a	.2889	14	12	2	13	11	3	001
661.13401	.2428	20	8	13	19	7	12	010
661.48313a	.3112	14	14	1	13	13	0	020
690.63052	.1557	19	9	11	18	8	10	010
691.37971a	.1349	18	13	6	17	12	5	100
698.46870a	.1818	24	9	16	23	8	15	000
698.77006b	.1111	23	9	15	22	8	14	000
699.65764b	.1152	18	14	5	17	13	4	100
722.37214a	.4364	17	16	1	16	15	2	010
722.91670a	.4218	17	17	0	16	16	1	010
770.08621a	.1778	21	11	10	20	10	11	010
771.40923	.6035	21	13	8	20	12	9	000
771.40923	.6035	19	16	4	18	15	3	010
771.75382a	.1903	19	19	1	18	18	0	010
773.63854a	.2553	19	17	3	18	16	2	010
773.83385a	.2216	19	18	2	18	17	1	010
783.29377a	.1945	20	14	7	19	13	6	010
784.21363	.1818	21	12	9	20	11	10	010
791.97967a	.1252	23	10	13	22	9	14	010
804.19000b	.1302	22	12	11	21	11	10	010
811.93309a	.2835	21	15	6	20	14	7	010
811.97965a	.1856	21	15	7	20	14	6	010
816.15525a	.1429	22	13	10	21	12	9	010
817.15695a	.1864	21	16	5	20	15	6	010
817.20881b	.1125	24	12	12	23	11	13	000
819.93233b	.2082	25	11	14	24	10	15	000
820.58322	.1585	21	17	5	20	16	5	010
822.18246b	.1162	21	19	2	20	18	3	010
822.26460b	.1341	21	18	3	20	17	4	010
864.04819	.1623	18	6	13	17	3	14	010
864.62304b	.1437	19	5	14	18	4	15	010
865.92987b	.1614	24	17	8	23	16	7	000
872.56591	.0764	24	22	3	23	21	2	000
872.97092	.1659	19	6	14	18	3	15	000
873.05353a	.1227	24	19	5	23	18	6	000

Note. Both new assignments for misassigned transitions and corrected frequencies for the old assignments are given. Some of the transitions, presented here for completeness, were ambiguously assigned in Ref. (3) (marked with asterisks in Ref. (3)). The present work eliminates the ambiguity. All wavenumbers are in cm⁻¹ and intensities in arbitrary relative units.

^a Lines reassigned from I.

^b Lines for which the assignments in I were ambiguous which can now be unambiguously assigned.

calculations as part of our project to construct a full line list of water transitions.

There is one qualitative aspect of the values of high K_a energy levels in water which should be mentioned. The appearance of fourfold, Type I, clusters in highly excited rotational states has been observed experimentally for H₂Se (18), but the structure of the levels was predicted to be significantly different in the ground vibrational state of water (5). Kozin and Jensen (19) rediscovered Type II clusters, first predicted by Lehmann (20), for (100) and (001) vibra-

TABLE 7
Pure Rotational Transitions Extending Our Assignments for the (000) and (010) States to Slightly Higher K_a Than in Ref. (3)

Wavenumber	Intensity	J'	K'_a	K'_c	J	K_a	K_c	$v_1v_2v_3$
819.93233	.2082	25	11	14	24	10	15	000
863.18595	.0570	24	24	1	23	23	0	000
869.07782	.0660	24	23	2	23	22	1	000
872.56591	.0764	24	22	3	23	21	2	000
873.05353	.1227	24	19	5	23	18	6	000
874.26301	.0858	24	21	4	23	20	3	000
733.79245	.2375	22	9	14	21	8	13	010
736.18371	.2552	21	8	13	20	7	14	010
736.64912	.2535	21	9	12	20	8	13	010
783.26340	.0802	20	14	6	19	13	7	010
783.29377	.1945	20	14	7	19	13	6	010
784.18819	.0778	21	12	10	20	11	9	010
784.21363	.1818	21	12	9	20	11	10	010
789.15380	.1598	22	11	12	21	10	11	010
794.37417	.1181	20	20	1	19	19	0	010
794.67518	.2074	20	16	5	19	15	4	010
804.19000	.1302	22	12	11	21	11	10	010
804.27309	.0507	22	12	10	21	11	11	010
804.86734	.0557	21	14	8	20	13	7	010
815.89698	.0848	21	21	0	20	20	1	010
816.15525	.1429	22	13	10	21	12	9	010
816.18551	.0491	22	13	9	21	12	10	010
817.15695	.1864	21	16	5	20	15	6	010
820.19016	.0965	21	20	1	20	19	2	010
822.18246	.1162	21	19	2	20	18	3	010
822.26460	.1341	21	18	3	20	17	4	010
825.76670	.1310	22	14	9	21	13	8	010
833.23378	.0340	22	15	7	21	14	8	010
833.52166	.0677	22	15	8	21	14	7	010
835.89141	.0339	23	13	11	22	12	10	010
836.00367	.0905	23	13	10	22	12	11	010
836.38869	.0416	22	22	1	21	21	0	010
838.87129	.1199	22	16	7	21	15	6	010
841.64931	.0433	22	21	2	21	20	1	010
842.77028	.0820	22	17	6	21	16	5	010
845.01762	.0726	22	18	5	21	17	4	010
845.63559	.0617	22	19	4	21	18	3	010
845.67541	.0643	23	14	9	22	13	10	010
845.98638	.0239	23	14	10	22	13	9	010
853.61240	.0225	23	15	9	22	14	8	010
853.81702	.0705	23	15	8	22	14	9	010
859.83868	.0687	23	16	7	22	15	8	010

Note. All wavenumbers are in cm⁻¹ and intensities in arbitrary relative units.

TABLE 8
Corrected List of Energy
Levels in cm^{-1} for the (010)
State

J	K_a	K_c	Position
17	7	11	6123.362
17	16	2	8651.288
17	17	0	8947.997
18	7	12	6546.756
18	17	2	9400.075
18	18	1	9695.959
19	16	3	9559.788
19	17	2	9869.930
19	18	1	10173.908
19	19	0	10467.713
20	14	7	9406.518
20	17	4	10357.339
20	18	3	10668.494
20	19	2	10971.516
20	20	1	11262.087
21	14	7	9897.582
21	15	6	10218.498
21	16	5	10540.670
21	17	4	10861.951
21	18	3	11179.604
21	19	2	11490.677
21	20	1	11791.702
21	21	0	12077.984

Note. Values were computed using the reassigned lines in Table 6 and lines from Table 7.

tional states of H_2X systems. Type II clusters were confirmed experimentally for H_2Se by Flaud *et al.* (21).

Initially, when we assigned the pure rotational lines of the (100) and (001) vibrational states and constructed the system of experimentally derived energy levels up to $J = 19$ (Fig. 1), we thought that we had found experimental evidence for Type II clustering for water. However, as in the case for Type I clusters for the ground state, it turns out that water is significantly different from the close analogs H_2S and H_2Se . For true clustering, the levels should move asymptotically closer together with increasing J . Instead, for $J = 20$ the levels cross; again water does not display the expected clustering behavior. Indeed, our calculated energy levels indicate continued divergence of (100) and (001) levels with increasing J .

IV. CONCLUSION

We have observed pure rotational difference band transitions in water. While estimates of the positions of most of the pure rotational transitions given in Table 4 appear in standard compilations of the water spectrum (16), rotational

difference transitions are absent. It would appear that this type of transition has been overlooked previously.

After overcoming the assignment problems associated with the rotational difference bands, we were able to significantly increase the number of assigned lines belonging to the (020) vibrational state. Lines involving levels up to $K_a = 18$ were assigned for (020). Previously only levels up to $K_a = 10$ were known for this state. We note that a few of the high K_a assignments of Toth (11) are not correct but those of Ref. (12) are in agreement with the work reported here and in Ref. (9). These new levels should be particularly sensitive to the potential at small $\text{H}\ddot{\text{O}}\text{H}$ angles and will therefore provide new information for the potential.

We expect rotational difference bands to be common in the rotational spectrum of hot water, in particular, and hot molecules in general. For example, we have already detected such bands in the (030), (011), and (110) water polyad (22).

ACKNOWLEDGMENTS

We thank H. Partridge and D. W. Schwenke for supplying their potential energy surface prior to publication. We thank L. Coudert for discussions on the assignments made in Ref. (3) and Per Jensen for critically reading the manuscript. The authors acknowledge NATO Grant 5-2-05/CRG951293 for making the experimental-theoretical collaboration possible. The work of O.L.P. was supported in part by the Russian Fund for Fundamental Studies. This work was supported by the Natural Sciences and Engineering Research Council of Canada (NSERC). Acknowledgment is made to the Petroleum Research Fund and the NASA laboratory astrophysics program for partial support of this work. Support was also provided by the UK Engineering and Science Research Council and the UK Particle Physics and Astronomy Research Council. We thank B. Winnewisser for her comments.

REFERENCES

1. L. Wallace, P. Bernath, W. Livingston, K. Hinkle, J. Busler, B. Guo, and K. Zhang, *Science* **268**, 1155–1158 (1995).
2. L. Wallace, W. Livingston, and P. F. Bernath, "An Atlas of the Sunspot Spectrum from 470 to 1233 cm^{-1} (8.1 to 21 μm) and the Photospheric Spectrum from 460 to 630 cm^{-1} (16 to 22 μm)," NSO Technical Report 1994-01, Tucson, AZ, 1994.
3. O. L. Polyansky, J. R. Busler, B. Guo, K. Zhang, and P. F. Bernath, *J. Mol. Spectrosc.* **176**, 305–315 (1996).
4. O. L. Polyansky, *J. Mol. Spectrosc.* **112**, 79–87 (1985).
5. O. L. Polyansky, P. Jensen, and J. Tennyson, *J. Chem. Phys.* **101**, 7651–7657 (1994).
6. O. L. Polyansky, P. Jensen, and J. Tennyson, *J. Chem. Phys.* **105**, 6490–6497 (1996).
7. N. F. Zobov, O. L. Polyansky, C. R. Le Sueur, and J. Tennyson, *Chem. Phys. Lett.* **260**, 381–385 (1996).
8. D. W. Schwenke, personal communication. Preliminary fit to the ab initio data of H. Partridge and D. W. Schwenke, *J. Chem. Phys.* **106**, 4618–4639 (1997).
9. O. L. Polyansky, N. F. Zobov, J. Tennyson, J. Lotoski, and P. F. Bernath, *J. Mol. Spectrosc.* **184**, 35–50 (1997).
10. J.-M. Flaud, C. Camy-Peyret, and J.-P. Maillard, *Mol. Phys.* **32**, 499–521 (1976).
11. R. A. Toth, *J. Opt. Soc. Am. B* **10**, 1526–1544 (1993).
12. S. N. Mikhailenko, V. I. G. Tuterev, K. A. Keppler, B. P. Winnewisser, M. Winnewisser, G. Mellau, S. Klee, and K. N. Rao, *J. Mol. Spectrosc.* **184**, 330–349 (1997).

13. K. Matsumura, T. Etoh, and T. Tanaka, *J. Mol. Spectrosc.* **90**, 106–115 (1981).
14. J.-M. Flaud and C. Camy-Peyret, *J. Mol. Spectrosc.* **51**, 142–150 (1974).
15. L. H. Coudert, private communication.
16. L. S. Rothman, R. R. Gamache, R. H. Tipping, C. P. Rinsland, M. A. H. Smith, D. C. Benner, V. Malathy Devi, J.-M. Flaud, C. Camy-Peyret, A. Perrin, A. Goldman, S. T. Massie, L. R. Brown, and R. A. Toth, *J. Quant. Spectrosc. Radiat. Transfer* **48**, 490–507 (1992).
17. J.-M. Flaud, C. Camy-Peyret, and R. A. Toth, "Water Vapour Line Parameters from Microwave to Medium Infrared," Pergamon Press, Elmsford, NY (1981).
18. I. N. Kozin, O. L. Polyansky, S. P. Belov, and M. Yu. Tretyakov, *J. Mol. Spectrosc.* **152**, 13–28 (1993).
19. I. N. Kozin and P. Jensen, *J. Mol. Spectrosc.* **161**, 186–207 (1993).
20. K. K. Lehmann, *J. Chem. Phys.* **95**, 2361–2370 (1991).
21. J.-M. Flaud, C. Camy-Peyret, H. Burger, P. Jensen, and I. N. Kozin, *J. Mol. Spectrosc.* **172**, 126–134 (1995).
22. O. L. Polyansky, N. F. Zobov, S. Viti, J. Tennyson, P. F. Bernath, and L. Wallace, *Science* **277**, 346–348 (1997).